

RESEARCH ARTICLE

Compressive force regulates orthodontic tooth movement via activating the NLRP3 inflammasome

Yineng Han^{1,2,3} | Qiaolin Yang^{1,3} | Yiping Huang^{1,3} | Pengfei Gao^{4,5} | Lingfei Jia^{3,6,7} | Yunfei Zheng^{1,3}  | Weiran Li^{1,3} 

¹Department of Orthodontics, Peking University School and Hospital of Stomatology, Beijing, People's Republic of China

²Key Laboratory of Oral Biomedical Research of Zhejiang Province, Stomatology Hospital, School of Stomatology, Zhejiang University School of Medicine, Zhejiang Provincial Clinical Research Center for Oral Diseases, Hangzhou, People's Republic of China

³National Center of Stomatology, National Clinical Research Center for Oral Diseases, National Engineering Laboratory for Digital and Material Technology of Stomatology, Beijing, People's Republic of China

⁴Key Laboratory of Cell Proliferation and Differentiation of the Ministry of Education, School of Life Sciences, Peking University, Beijing, People's Republic of China

⁵Peking-Tsinghua Center for Life Sciences, Beijing, People's Republic of China

⁶Department of Oral and Maxillofacial Surgery, Peking University School and Hospital of Stomatology, Beijing, People's Republic of China

⁷Central Laboratory, Peking University School and Hospital of Stomatology, Beijing, People's Republic of China

Correspondence

Yunfei Zheng and Weiran Li,
 Department of Orthodontics, Peking University School and Hospital of Stomatology, 22 Zhongguancun Avenue South, Haidian District, Beijing 100081, People's Republic of China.
 Email: yunfei_zheng@bjmu.edu.cn and weiranli@bjmu.edu.cn

Funding information

National Natural Science Foundation of China (NSFC), Grant/Award Number: 82071142 and 82071119

Abstract

Mechanical stress regulates various cellular functions like cell inflammation, immune responses, proliferation, and differentiation to maintain tissue homeostasis. However, the impact of mechanical signals on macrophages and the underlying mechanisms by which mechanical force regulates bone remodeling during orthodontic tooth movement remain unclear. NOD-like receptor family pyrin domain-containing 3 (NLRP3) inflammasome has been reported to promote osteoclastic differentiation to regulate alveolar bone resorption. But the relationship between the compressive force and NLRP3 inflammasome in macrophages remains unknown. In this study, immunohistochemical staining results showed elevated expression of NLRP3 and interleukin-1 β , as well as an increased number of macrophages expressing NLRP3, on the compression side of the periodontal tissues, after force application for 7 days. Furthermore, the number of tartrate-resistant acid phosphatase-positive osteoclasts, and the mRNA and protein

Abbreviations: AMPK, adenosine monophosphate-activated protein kinase; ANOVA, analysis of variance; ASC, apoptosis-associated speck-like protein containing a CARD; BMDMs, bone marrow-derived macrophages; cGAS, cyclic GMP-AMP synthase; CQ, chloroquine; FGFR2, fibroblast growth factor receptor 2; FoxO, Forkhead box; GAPDH, glyceraldehyde-3-phosphate dehydrogenase; GDF15, growth differentiation factor 15; H&E, hematoxylin and eosin; IL, interleukin; IRF3, interferon regulatory factor 3; LC3, light chain 3; LPS, lipopolysaccharide; M-CSF, macrophage colony stimulating factor; micro-CT, microcomputed tomography; NF- κ B, nuclear factor kappa light chain enhancer of B cells; NLRP3, NOD-like receptor family pyrin domain containing 3; OTM, orthodontic tooth movement; PCNA, proliferating cell nuclear antigen; PMA, phorbol 12-myristate 13-acetate; p-IRF3, phosphorylated interferon regulatory factor 3; P2X7R, purinergic 2X7 receptor; ROCK1, Rho-associated coiled-coil kinase 1; STING, stimulator of interferon response cGAMP interactor; TRAP, tartrate-resistant acid phosphatase; qRT-PCR, quantitative reverse-transcription polymerase chain reaction; YAP, Yes-associated protein; 3D, three-dimensional; 3-MA, 3-Methyladenine.

© 2022 Federation of American Societies for Experimental Biology.

expression levels of osteoclast-related genes in the periodontal tissue decreased in the *Nlrp3*^{-/-} mice compared to the WT mice group after orthodontic movement. In vitro mechanical force activates the NLRP3 inflammasome and inhibits autophagy. Intraperitoneal injection of the autophagy inhibitor 3-methyladenine in *Nlrp3*^{-/-} mice promoted orthodontic tooth movement. This result indicates that the absence of NLRP3 inflammasome activation can be partially compensated for by autophagy inhibitors. Mechanistically, force-induced activation of the NLRP3 inflammasome in macrophages via the cGAS/P2X7R axis. In conclusion, compressive force regulates orthodontic tooth movement via activating the NLRP3 inflammasome.

KEYWORDS

autophagy, cyclic GMP-AMP synthase, mechanical force, NLRP3 inflammasome, purinergic 2X7 receptor

1 | INTRODUCTION

Mechanical stimulation maintains tissue homeostasis and promotes tissue development by regulating bone remodeling and immune responses.¹ There are multiple types of mechanical stimuli like compressive force,² fluid flow,³ and tensile force.⁴ Mechanical stress affects various tissues, such as the periodontal ligaments, heart, lungs, bones, and intestines. Cells in these tissues play an important role in maintaining tissue homeostasis.⁵ In the tissues surrounding the alveolar bone, mechanical force leads to increased expression of chemokines and inflammatory cytokines. The mechanical force also activates immune cells, such as T lymphocytes and macrophages, that contribute to alveolar bone remodeling.^{6,7} Physiological mechanical stress maintains tissue homeostasis, whereas a lack of mechanical stress or excessive force leads to pathological changes. For example, periodontal tissue receiving excessive occlusal or orthodontic force promotes inflammatory responses and undermines bone resorption.⁸ In contrast, periodontal tissues that lose occlusal force stimulation induce the expression of inflammatory cytokines and cause periodontal ligament tissue degradation.⁹ Therefore, an optimal amount of mechanical force is required to maintain physiological homeostasis in the microenvironment. However, the specific mechanism by which mechanical stress contributes to alveolar bone remodeling remains unclear.

Mechanical stress leads to tooth movement by modulating the bone remodeling process. When a mechanical force is exerted on a tooth, the periodontal ligament undergoes aseptic inflammation, resulting in bone resorption on the compression side and bone accumulation on the tension side.¹⁰ Macrophages participate in the immune response by phagocytosing pathogenic microorganisms and

releasing inflammatory cytokines that induce an inflammatory response.¹¹ In addition, macrophages are precursors of osteoclasts, which participate in pro-inflammatory responses and bone remodeling during the orthodontic process.^{12,13} Previous studies have reported that periodontal ligament cells respond to mechanical stress.^{14,15} However, the effect of mechanical signals on macrophages remains unclear.

The NOD-like receptor family pyrin domain-containing 3 (NLRP3) inflammasome, a major innate immune sensor, comprises apoptosis-associated speck-like protein containing a caspase recruitment domain (ASC), NLRP3, and pro-caspase1. Two signals, the initial priming signal I and activation signal II, jointly activate the NLRP3 inflammasome. The nuclear factor kappa light chain enhancer of activated B cells (NF-κB) pathway is activated in priming signal I and subsequently increases the expression of pro-interleukin (IL)-1β, pro-IL-18, and pro-caspase1. The activation of the NF-κB pathway is initiated by several signals, including the toll receptor, tumor necrosis factor receptor, and the cyclic GMP-AMP synthase (cGAS)-stimulator of interferon response cGAMP interactor (STING) pathway. The cGAS-STING pathway is critical for immune responses against cancer and infections. STING activation triggers numerous signaling cascades that activate interferon regulatory factor 3 (IRF3), mitogen-activated protein kinase, NF-κB, and lysosome-dependent cell death.¹⁶ cGAS-STING-NLRP3 has been reported to be involved in bacterial infections in human myeloid cells.¹⁷ The activation signal II is triggered by pathogen-associated molecular patterns (PAMPs) and danger-associated molecular patterns (DAMPs), including the extracellular adenosine triphosphate (ATP)/purinergic2X7 receptor (P2X7R), nigericin, mitochondrial DNA, and so on. NLRP3 clustering of ASC triggers the oligomerization of pro-caspase1,

forming caspase1.¹⁸ Active caspase1 induces cleavage of pro-IL-1 β , pro-IL-18, and gasdermin D, resulting in their activation and secretion; the cytokines then recruit more effector cells to the infection site.¹⁹ Therefore, activated IL-1 β p17 is an important indicator of NLRP3 inflammasome activation. Monocytes/macrophages that differentiate into osteoclasts under specific conditions, express high levels of NLRP3.²⁰ Studies have shown that the NLRP3 inflammasome promotes osteoclastic differentiation in order to regulate alveolar bone resorption.²¹ Few studies have reported the regulatory mechanisms involved in the relationship between mechanical force and the NLRP3 inflammasome. One study reported that, in murine macrophages, cyclic tensile force suppressed the secretion of IL-1 β through the inhibition of the NLRP3 inflammasome signaling pathway.²² However, the relationship between compressive force and NLRP3 inflammasome signaling and underlying mechanisms in macrophages remains unknown.

In this study, force-induced tooth movement models were built in vivo, and compressive force was loaded in vitro to investigate the underlying mechanisms of compressive force and the NLRP3 inflammasome that cause alveolar bone remodeling.

2 | MATERIALS AND METHODS

2.1 | Animals

Male 8-week-old mice, NLRP3-deficient (*Nlrp3*^{-/-}) and wild-type (WT; C57BL/6), were used in this study. The *Nlrp3*^{-/-} mice were provided by the School of Life Sciences, Peking University (Haidian District, Beijing, China). C57BL/6 mice were obtained from WeiTong LiHua Co. (Beijing, China). Animals were kept under pathogen-free conditions that complied with the experimental standards and were provided with water and food. All animal experimental procedures were approved by the Peking University Animal Care and Use Committee (LA2020329) and conformed to the ARRIVE guidelines.

2.2 | Force-induced tooth movement model and the intervention group

The force-induced tooth movement model was built according to a previous study.¹⁴ Nickel-titanium coil springs were ligated from the incisors to the right maxillary first molar (Figure 1A,B), with the contralateral maxillary first molar serving as a control. The incisors were bonded using flowable resin (3M ESPE, St. Paul, MN, USA), providing a constant force of 30 g for 7 d.²³

For the intervention group, *Nlrp3*^{-/-} mice were separated into three groups. Vehicle (normal saline) or 3-methyladenine (3-MA; 30 mg/kg, Sigma-Aldrich, Saint Louis, MO, USA) was intraperitoneally injected every two days, starting one day before the seven days of the constant force application. The mice were euthanized using pentobarbital sodium. The maxilla was carefully removed from the surrounding tissues and fixed in 4% paraformaldehyde for 24 h before further analysis. A stereomicroscope (SWZ1000, Nikon, Tokyo, Japan) was used to observe tooth movement from the occlusal view. The tooth movement distance was measured from the midpoint of the mesial rim of the second molar to the midpoint of the distal rim of the first molar.¹⁴

2.3 | THP-1-derived macrophages culture treatment and mechanical loading

To induce differentiation into macrophages, THP-1 human monocytes (ATCCTIB-202) were treated with phorbol 12-myristate 13-acetate (PMA; 50 ng/ml, Sigma-Aldrich) for 24 h. For mechanical loading, a 1.5 g/cm² continuous compressive force was loaded, using cover glass and metallic balls, for 6, 12, and 24 h, as previously described (Figure S1).²⁴ The THP-1-derived macrophages from the control group were cultured without compression.

2.4 | Isolation and differentiation of murine bone marrow-derived macrophages (BMDMs)

The tibiae and femora were extracted from the WT and *Nlrp3*^{-/-} mice. Thereafter, the BMDMs were flushed with Roswell Park Memorial Institute (RPMI)-1640 medium (Gibco, Grand Island, NY, USA). Following red blood cell lysis, the BMDMs were resuspended in RPMI-1640 medium containing macrophage colony-stimulating factor (M-CSF; 30 ng/ml, R&D, Emeryville, MN USA), 1% penicillin, and 10% fetal bovine serum for 3 d at 37°C. The cells were harvested and grown overnight in a 6-well plate for the mechanical loading experiments.

2.5 | Quantitative reverse-transcription-polymerase chain reaction (qRT-PCR)

TRIzol reagent (Invitrogen, Carlsbad, CA, USA) was used for total cellular RNA extraction. cDNA was synthesized from 2 μ g of the extracted RNA using an RT kit (Takara Bio, Tokyo, Japan), and SYBR Green Master Mix (Roche Applied Science, Basel, Switzerland) was used to amplify it using

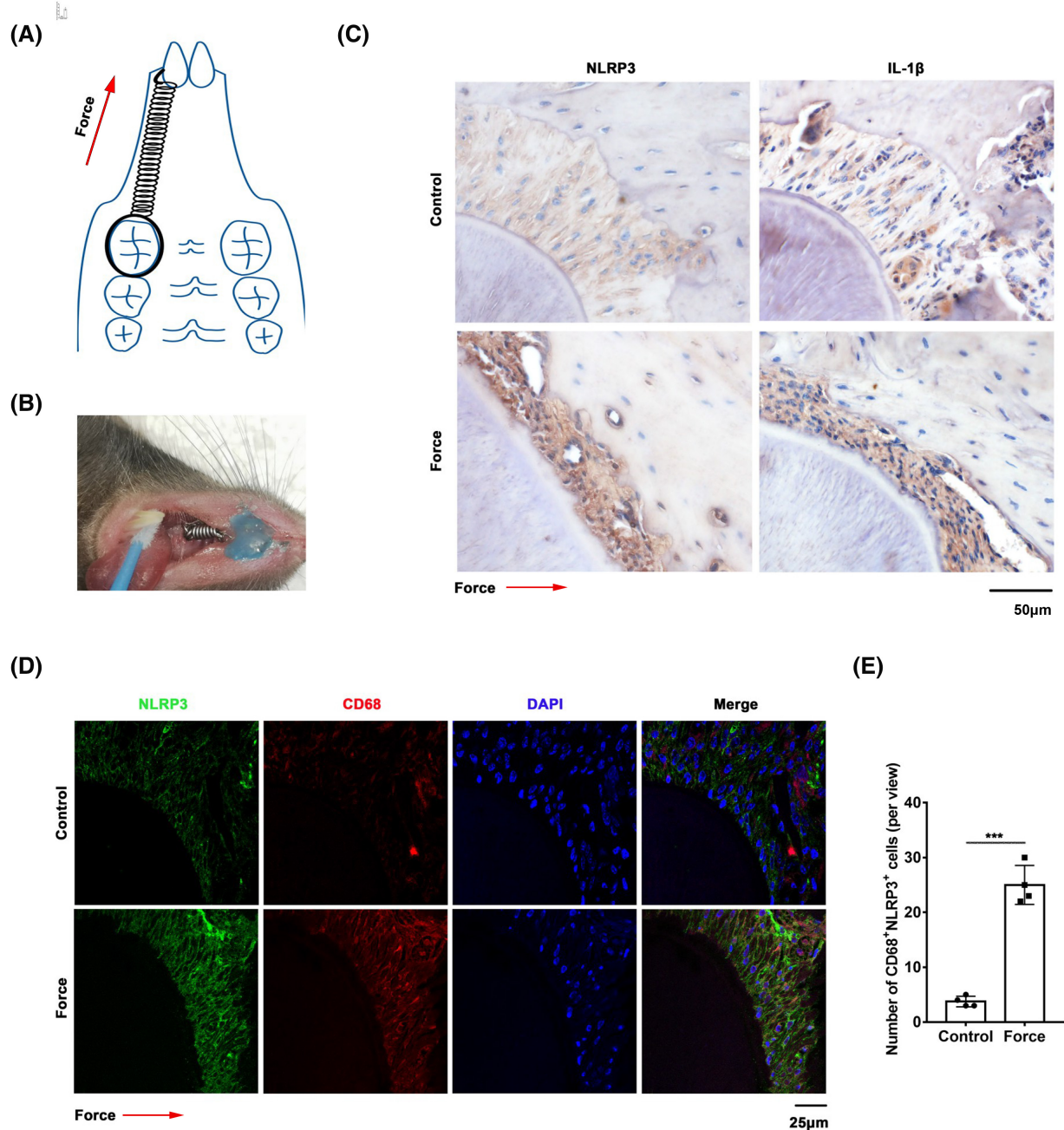


FIGURE 1 Force promotes NLRP3 expression in macrophages in vivo. (A) Diagrammatic sketch of mouse orthodontic tooth movement model. The coil spring was ligated between the left maxillary first molar and the left incisor. (B) Representative image of the experimental mouse orthodontic tooth movement procedures. (C) Immunohistochemistry staining (Scale bar = 50 μ m) of NLRP3 and interleukin (IL)-1 β in the control, force (compression side) groups ($n = 4$ /group). (D) Immunofluorescence double staining (Scale bar = 25 μ m) showing co-localization of CD68+ macrophages and NLRP3 expression in the control, force (compression side) groups. The arrow shows the direction of mechanical force. (E) The number of macrophages expressing NLRP3 (CD68 and NLRP3 co-localization) of the 400 \times magnification field of the control and force groups ($n = 4$ /group) (** $p < .001$).

qRT-PCR. The qRT-PCR was performed on the ABI Prism 7500 Real-Time PCR System (Applied Biosystems, Foster City, CA, USA). The housekeeping gene glyceraldehyde-3-phosphate dehydrogenase (GAPDH) served as an internal reference. Results were calculated using the $2^{-\Delta\Delta C_t}$ relative expression method. The primers used are listed in Table S1.

2.6 | Western blotting

Western blotting was performed as described previously.²⁴ Radioimmunoprecipitation assay (RIPA) lysis buffer (Solarbio, Beijing, China), which was supplemented with a protease inhibitor mixture (Roche

Applied Science), was used to extract total protein from cultured cells. Protein concentrations were measured using a Pierce BCA Protein Assay Kit (Thermo Scientific, Waltham, MA, USA). After blocking with 5% milk-Tris-buffered saline with Tween 20 (TBST) for 1 h, primary antibodies were used for incubation overnight at 4°C. The following day, TBST was used to wash the membranes thrice, and the membranes were incubated with their corresponding secondary antibodies for 1 h at room temperature. An enhanced chemiluminescence kit was used to visualize the protein bands, which were then quantified using the ImageJ software (<http://rsb.info.nih.gov/ij/>) (National Institutes of Health, Bethesda, MD, USA). The antibodies used were listed in Table S2.

2.7 | Micro-computed tomography (micro-CT) analysis

To measure the distance moved by the teeth, fixed mouse maxillae were scanned at a resolution of 10.8 μm using micro-CT (Skyscan1174, Bruker, Kontich, Belgium). To reconstruct the 3D images, NRecon and CTvox software were used.

2.8 | Hematoxylin and eosin (H&E) and tartrate-resistant acid phosphatase (TRAP) staining and

The specimens were decalcified by soaking them in ethylenediamine tetraacetic acid (10%, pH 7.4) for 14 d. The specimens were washed, dehydrated, and embedded in paraffin. Afterward, the 5- μm -thick sections were cut and stained with H&E according to a protocol from a previous study.⁶ A leukocyte acid phosphatase kit (387A-1KT; Sigma-Aldrich) was used for TRAP staining. A light microscope (Olympus, Tokyo, Japan) was used to capture the images of H&E- and TRAP-stained specimens; for TRAP-stained specimens, only TRAP-positive cells (having >2 nuclei) attached to the surface of the adjacent alveolar bone were considered.

2.9 | Immunofluorescence staining and immunohistochemical staining

For cell immunofluorescence staining, cells were fixed in 4% paraformaldehyde and permeabilized with 0.1% Triton X-100 at room temperature for 10 min. The cells were then incubated with 5% normal goat serum for 40 min at room

temperature and subsequently incubated with primary antibody at 4°C overnight. Next, they were incubated with the secondary antibody in dark at room temperature for 1 h. After incubation, 4', 6-diamidino-2-phenylindole (DAPI) (Solarbio) was used to counterstain the nuclei. A confocal laser scanning microscope (Carl Zeiss, Jena, Germany) was used for the visualization of the stained cells.

For tissue immunofluorescence staining, sections were blocked in 5% goat serum and then incubated with primary antibodies at 4°C overnight. Next, they were incubated with the secondary antibody in dark at room temperature for 1 h. DAPI (Solarbio) was used to counterstain the nuclei. The stained specimens were visualized using a confocal laser scanning microscope (Carl Zeiss). For immunohistochemical staining, proper secondary antibodies (ZSGB-Bio, Beijing, China) were applied and a DAB detection kit (ZSGB-Bio) was used for the production of a brown precipitate. The sections were counterstained with hematoxylin. The antibodies used were listed in Table S2.

2.10 | Statistical analysis

SPSS v.19.0 (IBM, Chicago, IL, USA) was used for statistical analysis. All data were expressed as the mean \pm standard deviation of at least three independent experiments. Parametric data underwent two-tailed unpaired Student's *t*-tests for two-group comparisons. One-way analysis of variance (ANOVA) was used for multiple group comparisons. The Mann-Whitney test was used for two-group comparisons of non-parametric data; the Kruskal-Wallis test for multigroup comparisons; and Tukey's multiple comparisons test for post hoc tests. Differences were considered statistically significant at a *p*-value < .05.

3 | RESULTS

3.1 | Force promotes NLRP3 expression in macrophages in vivo

We first established a murine model of orthodontic tooth movement (OTM) to test NLRP3 expression and downstream IL-1 β expression during OTM. Immunohistochemical staining revealed increased expression of NLRP3 and IL-1 β in the periodontal tissues on the compression side after applying force for 7 d (Figure 1C). Immunofluorescence staining results revealed more macrophages (CD68+) expressing NLRP3 on the compression

side of the periodontal tissues than in the control group (Figure 1D,E).

3.2 | Force-induced osteoclastogenesis is attenuated in *Nlrp3*^{-/-} mice

We measured the distance of tooth movement in the WT and *Nlrp3*^{-/-} mice. Increased tooth movement distances were observed in the OTM models compared with the control group. Intraoral photographs and micro-CT reconstruction images showed that the distances were significantly longer in the WT OTM group than in the *Nlrp3*^{-/-} OTM group (Figure 2A,B). TRAP staining results demonstrated that the area of TRAP-positive osteoclasts on the compression side of the periodontal tissue was markedly elevated after 7 days of the continuous force application. The *Nlrp3*^{-/-} OTM group had less area of TRAP-positive osteoclasts than the WT group (Figure 2A,C). In addition, the mRNA expression levels of osteoclast-related genes, TRAP, cathepsin K (CTSK), and matrix metalloproteinase 9 (MMP9) were lower in the *Nlrp3*^{-/-} OTM group than in the WT OTM group (Figure 2D). Moreover, TRAP protein expression in the *Nlrp3*^{-/-} OTM group was lower than that in the WT OTM group (Figure 2E).

3.3 | Force activates the NLRP3 inflammasome in macrophages

Next, we explored the influence of force on NLRP3 inflammasome-mediated osteoclastogenesis. After PMA treatment for 24 h, THP-1 cells, which are round suspension cells, differentiated into adherent M0 macrophages, which were polygonal and had long pseudopods. Western blotting results demonstrated that compressive force activated the NLRP3 inflammasome with the activation of caspase1 (p20) and release of activated IL-1 β (p17), both in whole-cell lysates (WCL) and culture supernatants (Sup) (Figure 3A,B).

3.4 | Force reduces autophagy by activating NLRP3 inflammasome in macrophages

Autophagy is a cellular response that occurs when a compressive force is applied to human periodontal ligament cells.^{25,26} In our experiment, the application of force reduced the expression levels of light chain 3 (LC3) II/I and Beclin1 in a time-dependent manner in THP-1-derived macrophages (Figure 3C,D). Moreover,

immunofluorescence staining results showed that the protein expression of LC3 I and Beclin1 significantly decreased with the application of force compared with the controls (Figure 3E). Next, we measured autophagic flux using a previously reported approach to distinguish between the inhibited synthetic and enhanced degradative phases of autophagy.²⁷ Chloroquine (CQ), which neutralizes lysosomal and vacuolar Ph, was used to block autophagic degradation. The western blotting result showed treatment with CQ to inhibit autophagy degradative phases did not further increase the LC3 II/I ratio after force application in THP-1-derived macrophages, indicating that mechanical compressive force impairs autophagosome synthesis (Figure S2). After that, we explored the role of NLRP3 in compressive force-reduced autophagy. Western blotting showed that NLRP3 was successfully knocked out in NLRP3^{-/-} THP-1-derived macrophages (Figure S3A). We found that NLRP3 knockout significantly increased force-reduced autophagy in both BMDMs from *Nlrp3*^{-/-} mice and NLRP3^{-/-} THP-1-derived macrophages, with elevated Beclin1 expression and increased transition of LC3 I to LC3 II (Figure 4A–D). Moreover, in vivo experiment showed that compressive force reduced autophagy on the compressive side and the expression of LC3 was higher in the *Nlrp3*^{-/-} OTM group compared with the WT OTM group (Figure S4).

3.5 | Force-induced OTM via NLRP3/autophagy-mediated osteoclastogenesis

Next, autophagy inhibitor 3-MA was intraperitoneally injected every 2 days in *Nlrp3*^{-/-} mice to investigate whether 3-MA can partially increase the attenuated tooth movement in *Nlrp3*^{-/-} mice via downregulating the autophagy level and whether compressive force regulates osteoclastogenesis via NLRP3/autophagy pathway. 3-MA is a widely used inhibitor of autophagy via its inhibitory effect on class III PI3K.²⁸ Immunohistochemical staining results showed that the expression of LC3 was decreased in the periodontal tissues on the compression side after applying force for 7 d, and the injection of 3-MA further increased autophagic dysfunction (Figure S5). Intraoral photographs and micro-CT results demonstrated increased OTM after the injection of 3-MA in *Nlrp3*^{-/-} mice compared with the *Nlrp3*^{-/-} OTM group (Figure 5A,B). There was an increased percentage of TRAP-positive osteoclast area and higher expression of TRAP in *Nlrp3*^{-/-} mice injected with 3-MA than in the *Nlrp3*^{-/-} OTM group (Figure 5A,C,D). The mRNA expression levels of osteoclast-related genes in the *Nlrp3*^{-/-} mice from the 3-MA injection group were higher than those in the

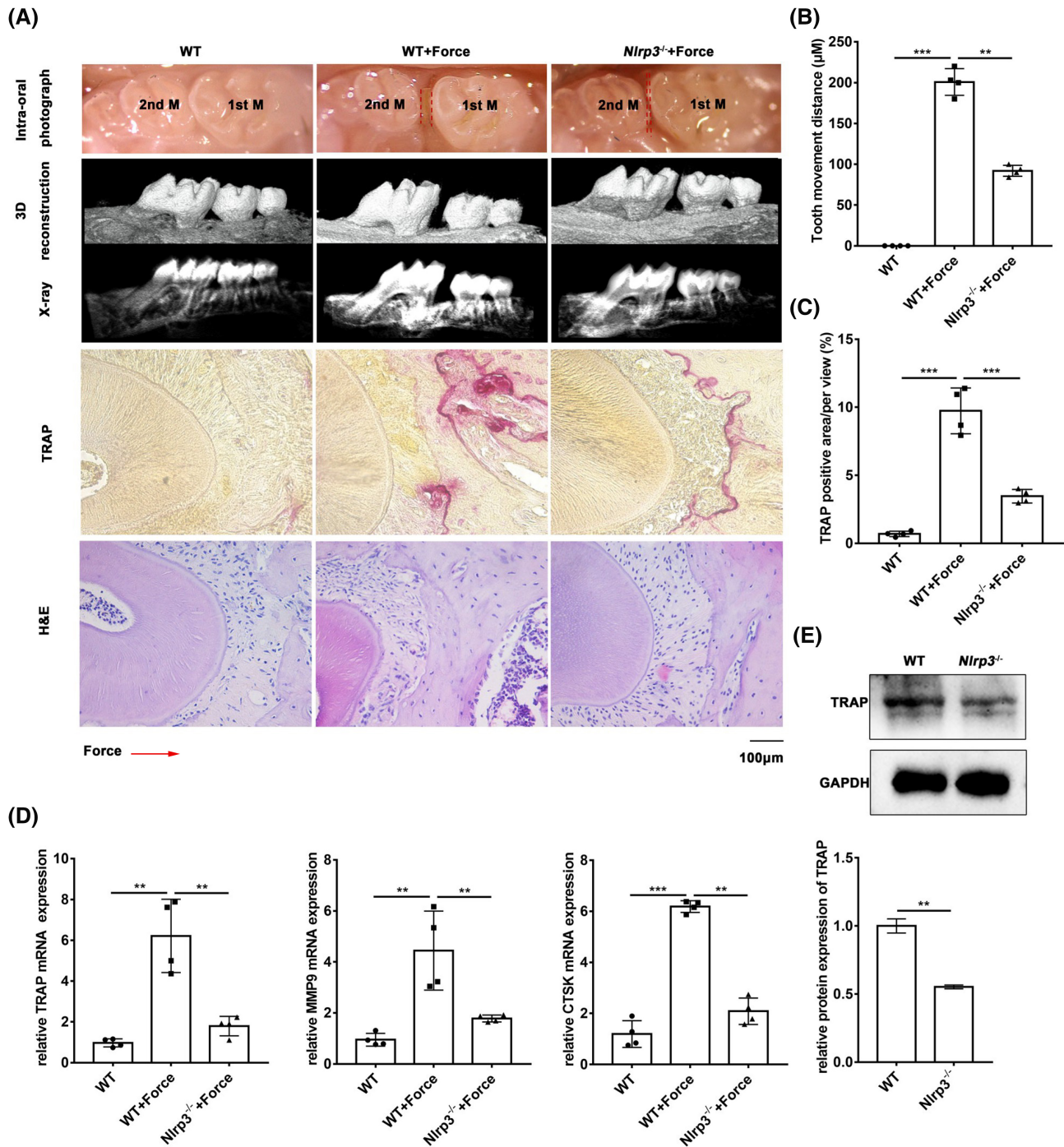


FIGURE 2 Force-induced osteoclastogenesis is attenuated in *Nlrp3*^{-/-} mice. (A) Representative intra-oral photograph, microcomputed tomography (micro-CT) images, tartrate-resistant acid phosphatase (TRAP), and hematoxylin and eosin (H&E) staining of tooth movement for 7 days of the force application. The arrow shows the direction of mechanical force. Scale bar = 100 µm. (B) Semiquantification analysis of the tooth movement distance between the upper first and second molar in WT, WT+Force, *Nlrp3*^{-/-}+Force groups (*n* = 4/group). (C) The percentage of TRAP-positive osteoclasts area on the compression side (*n* = 4/group). (D) mRNA expressions of TRAP, matrix metalloproteinase 9 (MMP9), and cathepsin K (CTSK) of the periodontal tissues in WT, WT+Force, *Nlrp3*^{-/-}+Force groups (*n* = 4/group). (E) Protein expressions of TRAP of the periodontal tissues in WT, WT+Force, *Nlrp3*^{-/-}+Force groups. Histogram shows the quantification of band intensities. GAPDH was used for normalization (***p* < .01, ****p* < .001).

Nlrp3^{-/-} OTM group (Figure 5E). These results indicated force-induced osteoclastogenesis via the NLRP3/autophagy pathway. The lack of NLRP3 inflammasome

activation, which inhibits osteoclastogenesis during OTM, can be partially compensated for by autophagy inhibitors.

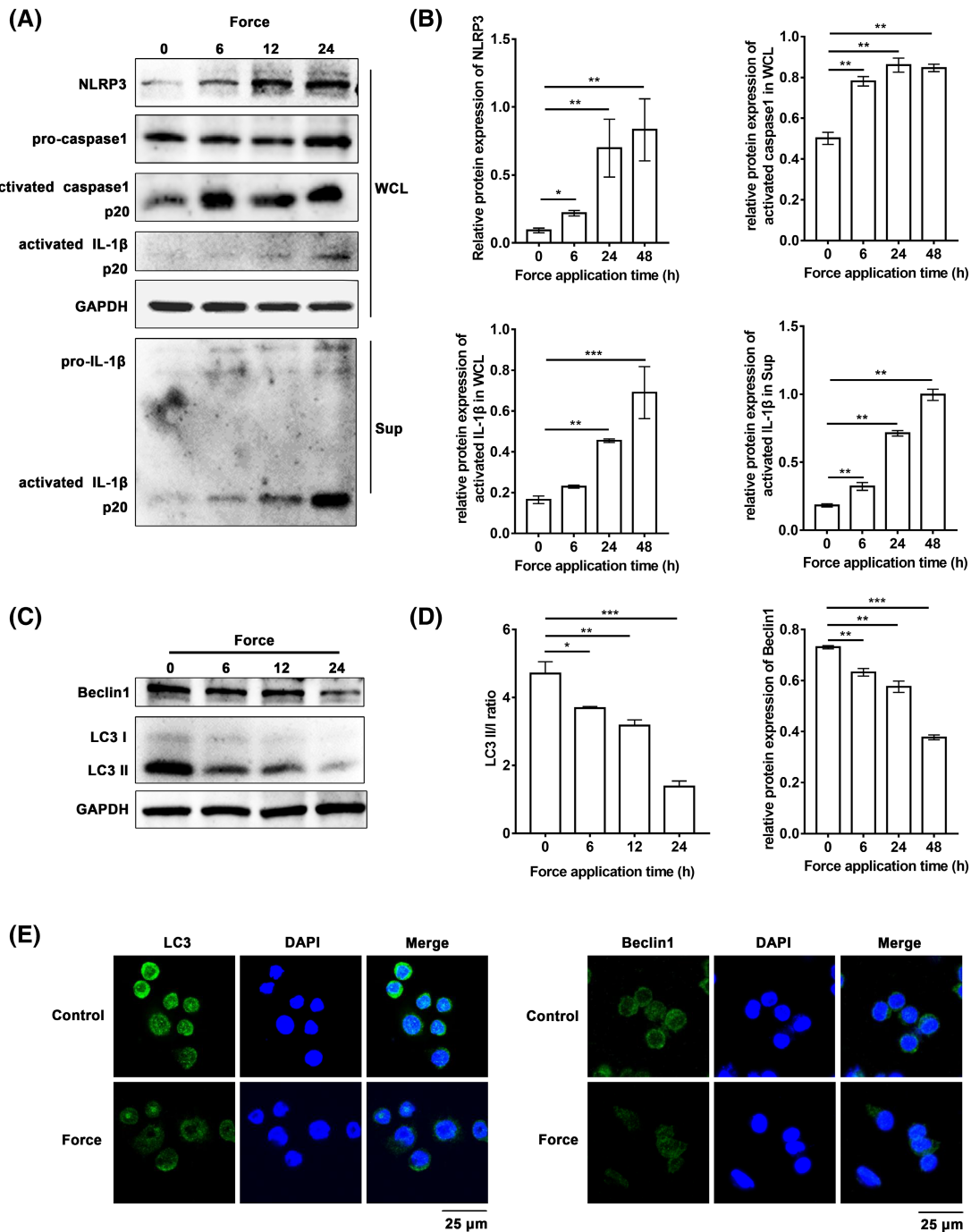


FIGURE 3 Compressive force activates NLRP3 inflammasome and reduces autophagy. (A and B) Protein expression of NLRP3, pro-caspase1, activated caspase1 (p20), pro-interleukin (IL)-1 β and activated IL-1 β (p17) in THP-1-derived macrophages with force application. Histograms show the quantification of band intensities and GAPDH was used for normalization. (C and D) Protein expression of Beclin1 and light chain 3 (LC3) II/I with force application. The histograms show the ratio of LC3 II/I and the quantification of band intensities. GAPDH was used for normalization. (E) Immunofluorescence staining of LC3 and Beclin1 in THP-1-derived macrophages with or without force application. Scale bar = 25 μ m (* $p < .05$, ** $p < .01$, *** $p < .001$).

3.6 | Compressive force activates the NLRP3 inflammasome via the cGAS-STING-NF- κ B-P2X7R signaling pathway

Finally, we explored the mechanisms underlying the activation of the NLRP3 inflammasome by compressive

force. The DNA sensor cGAS has been reported to be activated by endogenous DNA.¹⁶ In this study, we hypothesized that the cGAS-STING axis acts as a priming signal to activate the NF- κ B signaling pathway. Firstly, western blotting showed that cGAS was successfully knocked out in cGAS^{-/-} THP-1-derived macrophages (Figure S3B).

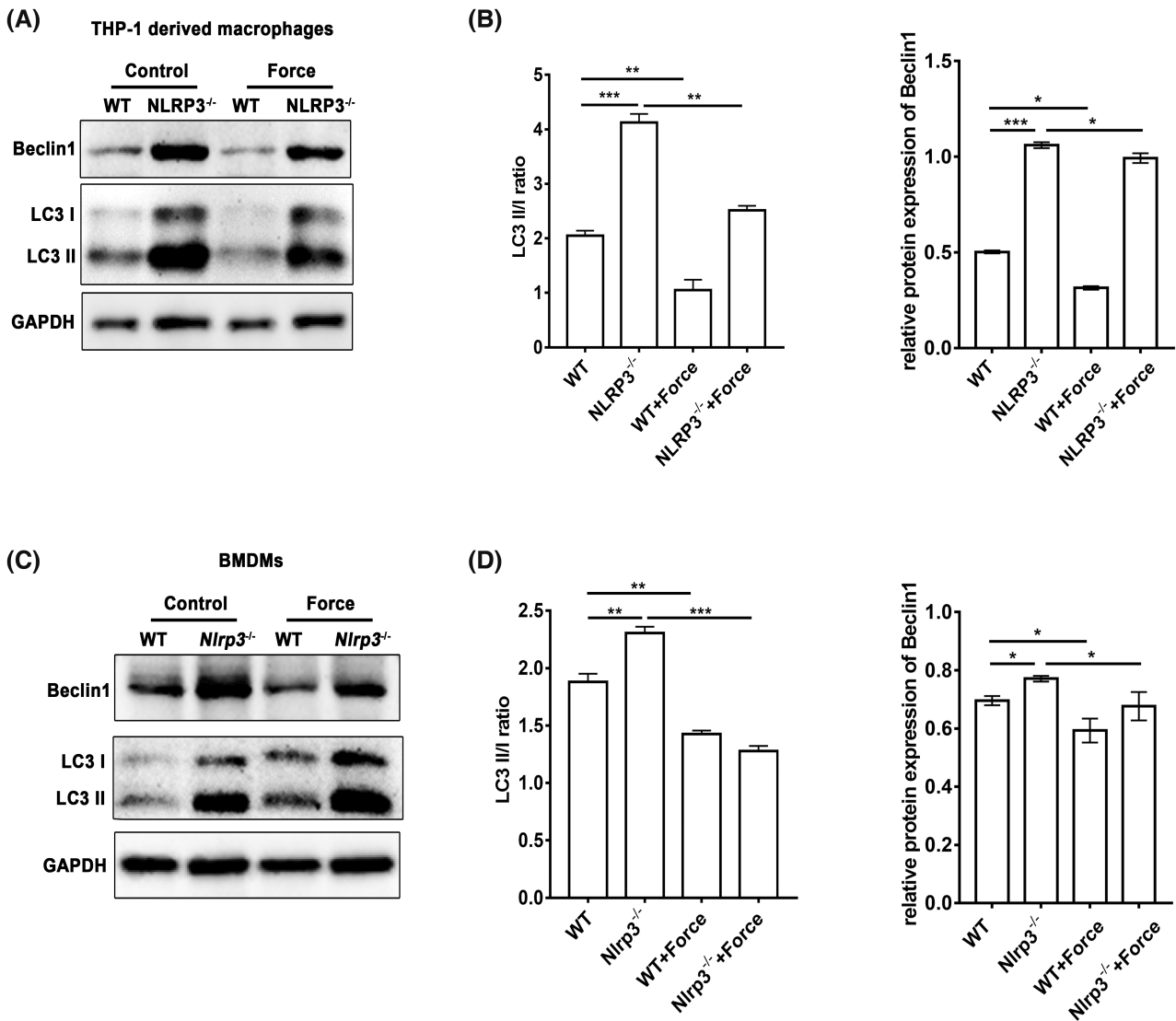


FIGURE 4 *NLRP3* knockout increases force-reduced autophagy. (A and B) Protein expression of Beclin1 and LC3 II/I in WT and *NLRP3*^{-/-} THP-1-derived macrophages with or without force application. The histograms show the ratio of LC3 II/I and the quantification of band intensities. GAPDH was used for normalization. (C and D) Protein expression of Beclin1 and LC3 II/I in BMDMs generated from WT and *Nlrp3*^{-/-} mice with or without force application. The histograms show the ratio of LC3 II/I and the quantification of band intensities. GAPDH was used for normalization (**p* < .05, ***p* < .01, ****p* < .001).

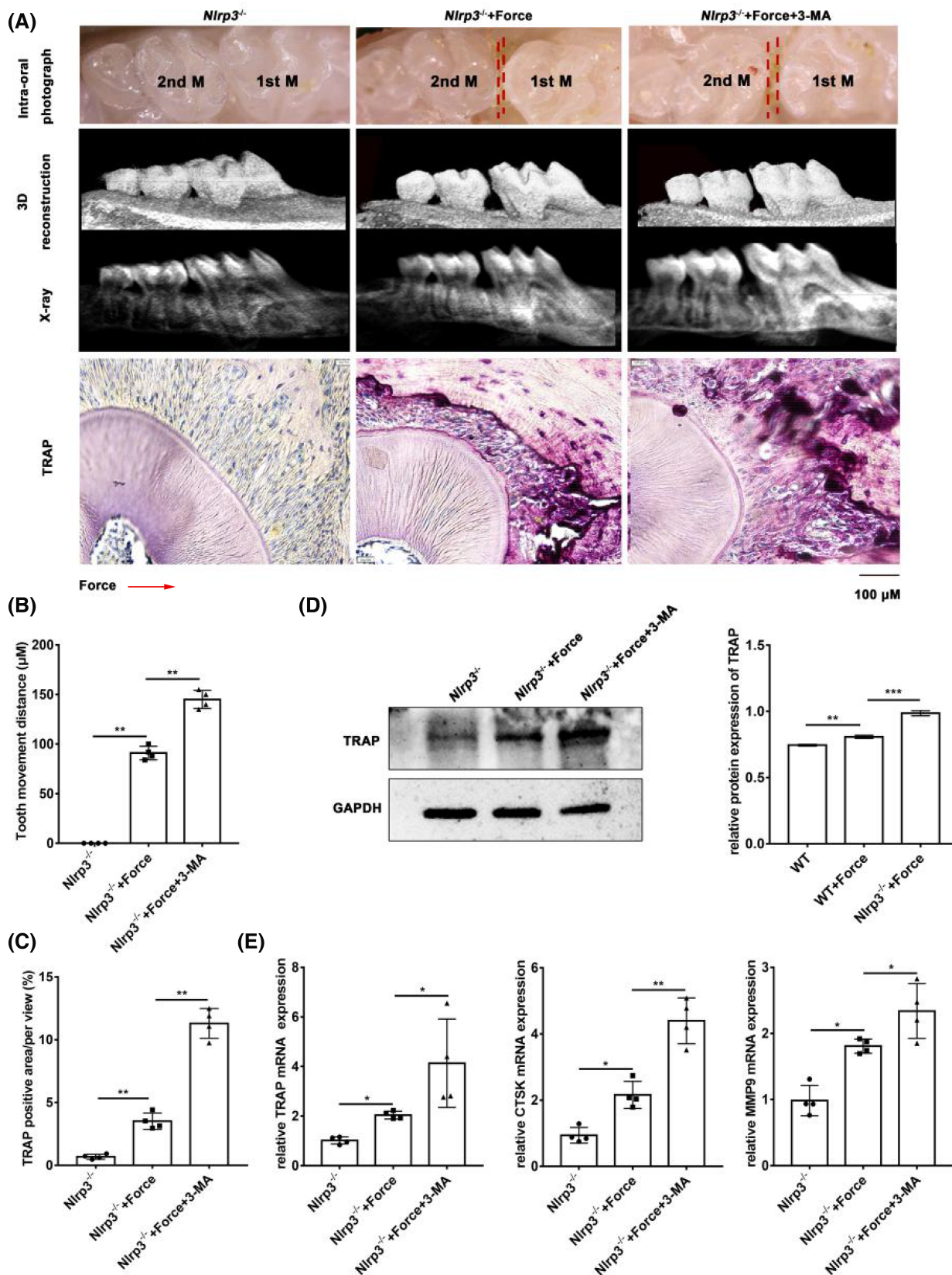
Compressive force activated NLRP3 inflammasome in WT THP-1-derived macrophages while in *cGAS*^{-/-} THP-1-derived macrophages, this activation effect was remarkably decreased (Figure 6A,D). Moreover, the activation of phosphorylated interferon regulatory factor 3 (p-IRF3) and NF- κ B was significantly inhibited in *cGAS*^{-/-} THP-1-derived macrophages after force application (Figure 6B,F). Immunofluorescence staining further showed that knockout of *cGAS* decreased the translocation of the NF- κ B p65 subunit from the cytoplasm to the nucleus after the application of force in THP-1-derived macrophages (Figure 6C,E).

P2X7R is closely related to mechanical force.²⁹ Therefore, we investigated whether compressive force activated the NLRP3 inflammasome via P2X7R. Western blotting showed that NLRP3 inflammasome activation was

significantly inhibited by the P2X7R inhibitor A-740003 (Figure 6G,H). These data suggest that mechanical force activates the NLRP3 inflammasome to regulate bone remodeling via a *cGAS*/P2X7R/autophagy-mediated mechanism.

4 | DISCUSSION

The mechanical force has an effect on various cell types, including macrophages, and is essential to maintaining tissue homeostasis. Macrophages, one of the major cell types in the periodontium, play a vital role in mediating mechanical load-induced inflammatory processes and bone remodeling. Previous studies have reported that tensile forces suppress osteoclast differentiation and fusion,⁴ whereas compressive



force promotes osteoclast differentiation and activation.² The NLRP3 inflammasome is involved in regulating osteoclastogenesis. Loss of NLRP3 has been reported to attenuate osteopenia in aging mice.³⁰ The NLRP3 inflammasome has

also been shown to regulate alveolar bone loss by promoting osteoclastic differentiation through IL-1 β production in periodontitis.³¹ One study reported that cyclic stretch on the periodontal ligament has been shown to induce NLRP1 and

FIGURE 5 Reduced osteoclastogenesis in *Nlrp3*^{-/-} mice is rescued by autophagy inhibitor 3-MA. (A) Representative intro-oral photograph, microcomputed tomography (micro-CT) images, tartrate-resistant acid phosphatase (TRAP) staining of tooth movement for 7 days in *Nlrp3*^{-/-}, *Nlrp3*^{-/-}+Force, *Nlrp3*^{-/-}+Force+3-MA groups. The arrow shows the direction of mechanical force. Scale bar = 100 μm. (B) Semiquantification analysis of the tooth movement distance between the upper first and second molar in *Nlrp3*^{-/-}, *Nlrp3*^{-/-}+Force, *Nlrp3*^{-/-}+Force+3-MA groups. (*n* = 4/group). (C) The number of TRAP-positive osteoclasts on the compression side in *Nlrp3*^{-/-}, *Nlrp3*^{-/-}+Force, *Nlrp3*^{-/-}+Force+3-MA groups. (*n* = 4/group). (D) Protein expressions of TRAP of the periodontal tissues in mice in *Nlrp3*^{-/-}, *Nlrp3*^{-/-}+Force, *Nlrp3*^{-/-}+Force+3-MA groups. Histogram shows the quantification of band intensities and GAPDH was used for normalization. (E) mRNA expressions of TRAP, matrix metalloproteinase 9 (MMP9), and cathepsin K (CTSK) of the periodontal tissues in *Nlrp3*^{-/-}, *Nlrp3*^{-/-}+Force, *Nlrp3*^{-/-}+Force+3-MA groups. (*n* = 4/group) (**p* < .05, ***p* < .01, ****p* < .001).

3 activation.³² While another study found that cyclic tensile force inhibits NLRP3 inflammasome-dependent IL-1β secretion via adenosine monophosphate-activated protein kinase (AMPK) signaling in murine macrophages.²² The different results may be because of different cell types, different force application times, and different force magnitudes. However, how compressive force regulates NLRP3 inflammasome remains unclear. In our study, we found that compressive force activated NLRP3 inflammasome and after force application, fewer TRAP-positive osteoclasts appeared on the compression side in the *Nlrp3*^{-/-} OTM group than in the WT OTM group.

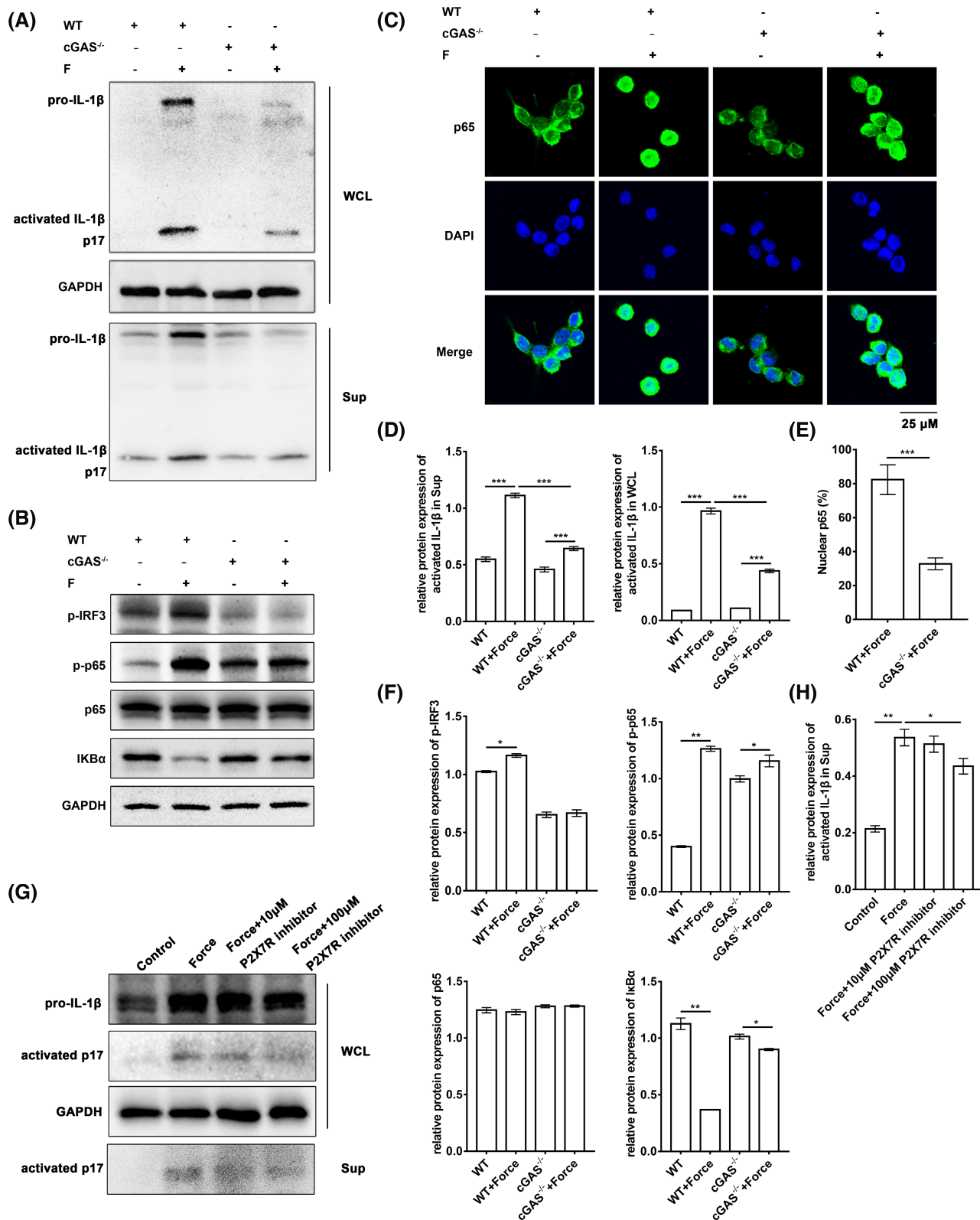
Several regulatory mechanisms have already been proposed as mediators of alveolar bone remodeling due to mechanical stress. Compressive force responsive gene growth differentiation factor 15 (GDF15) regulates orthodontic tooth movement via the Yes-associated protein (YAP)/GDF5/NF-κB axis under compressive force contributes to osteoclast differentiation in human periodontal ligament cells.³³ Cyclic strain is reported to cause the phosphorylation and retention in the cytoplasm of Forkhead box (FoxO) family members, increasing ERK kinase phosphorylation and proliferating cell nuclear antigen (PCNA) expression.³⁴ Aberrantly expressed miRNAs also participate in regulating orthodontic tooth movement. Compressive force inhibits osteoblast proliferation by upregulating miR-494-3p, which suppresses fibroblast growth factor receptor 2 (FGFR2) and Rho-associated coiled-coil kinase 1 (ROCK1) expression.³⁵ Expression of miR-29 in periodontal ligament cells is altered by compressive force, which affects several genes encoding major extracellular matrix components including Col1a1, Col3a1, and Col5a1.³⁶ In the present study, we found that we found that mechanical force activated the NLRP3 inflammasome via the cGAS/P2X7R pathway and elevated mature IL-β expression.

The cGAS-STING signal axis includes the synthesis of the second messengers cGAS and STING, which detect pathogenic DNA to trigger innate immune responses. As a DNA sensor, cGAS can also be activated by endogenous DNA, such as DNA released by the mitochondria and extranuclear chromatin produced by genotoxic stress, in addition to sensing microbial DNA. The cGAS-STING pathway is regarded as a critical signaling axis in sterile inflammation,

aging, and autoimmunity.³⁷ However, the relationship between mechanical force stimulation and cGAS-STING has not yet been reported. In this study, we found that mechanical stress activated the NF-κB pathway, indicating that mechanical force activates the priming signal of the NLRP3 inflammasome via the cGAS-STING pathway.

Following the efflux of K⁺ through the open channel, P2X7R serves as a second signal to activate the NLRP3 inflammasome.³⁸ Besides mediating NLRP3 inflammasome activation, P2X7R is also involved in T-lymphocyte survival and differentiation, cytokine and chemokine release, transcription factor activation, and cell death.³⁹ In addition, another study reported that root resorption was considerably more severe after orthodontic force application in P2X7R-knockout mice than in WT mice,²⁹ suggesting that P2X7R plays an important role in mechanotransduction; however, the underlying mechanism remains unclear. A recent study has reported that P2X7R mediates both steps of NLRP3 inflammasome activation in astrocytes exposed to mechanical strain, suggesting an important function in connecting mechanical strain to neuroinflammation.⁴⁰ In our study, we found that mechanical loading activated the NLRP3 inflammasome through P2X7R and partially reduced the maturation of IL-1β, indicating that mechanical force activates the NLRP3 inflammasome through different activation signals.

Autophagy is an intracellular process that is important for recycling damaged proteins and cell organelles, as well as the destruction of pathogens. Dysfunction of autophagy causes inflammatory diseases, such as inflammatory bowel disease, that are characterized by excessive inflammasome activation and excessive inflammation.⁴¹ The effects of tooth movement on autophagy in vivo are controversial. Jacox et al reported that orthodontic force activates macrophage autophagy in a force-dependent manner.⁴² Studies also found that administration of 3-MA upregulated osteoclasts and promoted OTM while administration of rapamycin, an autophagy activator, led to reduced OTM and osteoclast recruitment.^{26,43} Our previous study found that compressive force-induced lincRNA-p21 inhibits the mineralization of cementoblasts by impeding autophagy.⁴⁴ Altered degree of autophagic activation may be because of different force application time and magnitude, as well as different cell types, contributing to keeping bone homeostasis. In the present



study, we found that compressive force inhibited autophagy in vitro and in vivo, and administration of 3-MA in *Nlrp3*^{-/-} mice increased OTM.

Regulation of NLRP3 inflammasome activation and autophagy is important for maintaining hemostasis during mechanical stimulation. Some studies have reported that

overexpression of NLRP3 inflammasome core molecules increases autophagy and LC3 II protein expression in human macrophages infected with *Pseudomonas aeruginosa*.⁴⁵ Silencing of NLRP3 downregulated monosodium urate-induced autophagy and the conversion of LC3 I to LC3 II in osteoblasts.⁴⁶ In contrast, other studies have reported that the

FIGURE 6 Compressive force activates the NLRP3 inflammasome via cyclic GMP-AMP synthase (cGAS)-stimulator of interferon response cGAMP interactor (STING)-NF- κ B-purinergic 2X7 receptor (P2X7R) signaling pathway. (A and D) Protein expression of pro-interleukin (IL-1 β) and activated IL-1 β (p17) in WT, cGAS^{-/-} THP-1-derived macrophages with or without force application. Histograms show the quantification of band intensities and GAPDH was used for normalization. (B and F) Protein expression of phosphorylated interferon regulatory factor 3 (p-IRF3), phosphorylated-p65 (p-p65), p65 and inhibitory κ B protein (κ B)- α in WT, cGAS^{-/-} THP-1-derived macrophages with or without force application. Histograms show the quantification of band intensities and GAPDH was used for normalization. (C) Immunofluorescence staining of p65 in WT, cGAS^{-/-} THP-1-derived macrophages with or without force application. Scale bar = 25 μ m. (E) Quantification of p65 nuclear translocation percentage of the 400 \times magnification field of the WT and cGAS^{-/-} THP-1-derived macrophages with force application. (G and H) Protein expression of pro-IL-1 β and activated IL-1 β (p17) in control, Force, Force+10 μ M P2X7R inhibitor, Force+100 μ M P2X7R inhibitor groups. Histogram shows the quantification of band intensities and GAPDH was used for normalization (* p < .05, ** p < .01, *** p < .001).

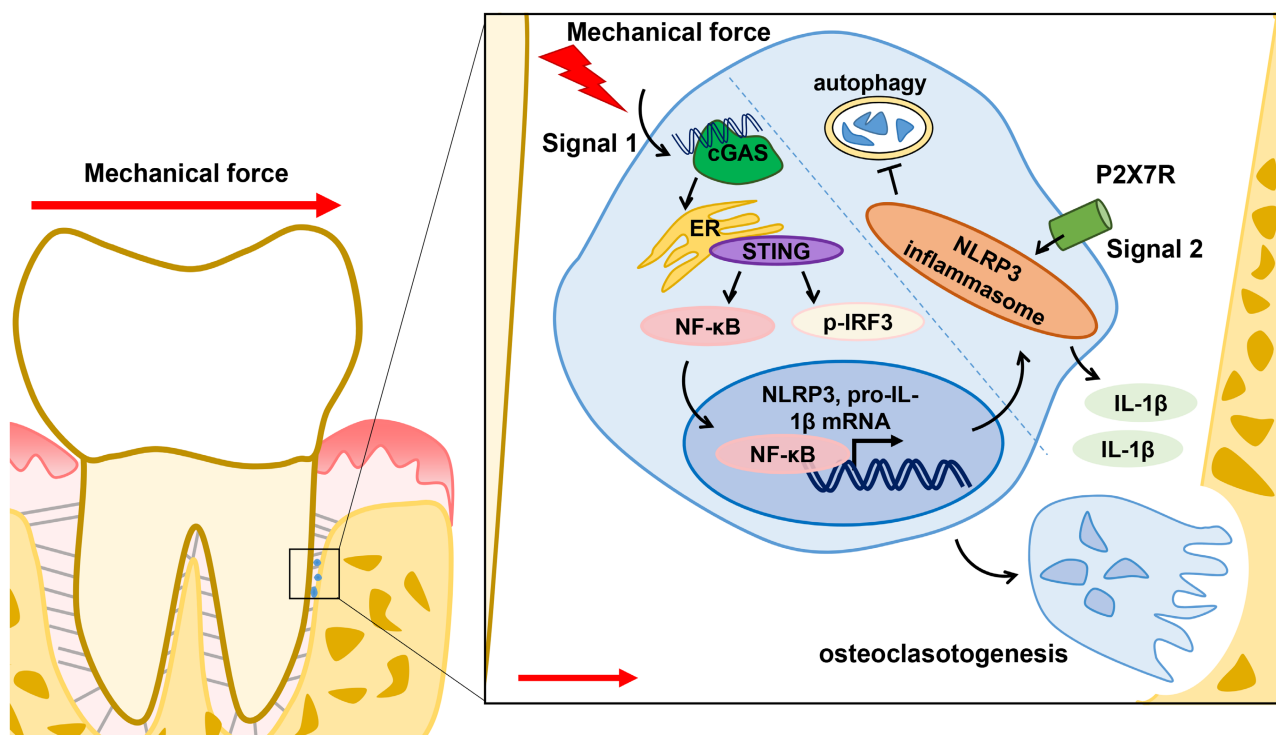


FIGURE 7 Schematic diagram showing mechanical force activates NLRP3 inflammasome to regulate bone remodeling via a cGAS/P2X7R/autophagy-mediated mechanism.

NLRP3 inflammasome negatively regulates the autophagic process in microglia after stimulation with NLRP3 inflammasome activator neurotoxic prion peptide PrP106-126.⁴⁷ One study reported that *Nlrp3*^{-/-} mice showed increased levels of autophagy under baseline and stress conditions, such as hypoxia.^{48,49} The discrepancies observed in the regulation of NLRP3 inflammasomes and autophagy in different studies may be attributed to the different NLRP3 inflammasome activators. Consistent with other previous studies, we found that NLRP3 deficiency promoted autophagy at baseline and during mechanical stimulation with a compressive force. The NLRP3 inflammasome has been reported to regulate autophagy by interacting with Beclin1 through the NACHT domain. Caspase1 also regulates autophagy by cleaving Parkin and Toll/IL-1 receptor domain-containing adapter-inducing interferon- β (TRIF).⁵⁰ In the present study, reduced osteoclastogenesis in *Nlrp3*^{-/-} mice

was compensated for by the autophagy inhibitor 3-MA, indicating that the lack of NLRP3 inflammasome activation, which inhibits osteoclastogenesis during OTM, can be partially increased by autophagy inhibitors. Regulation of the NLRP3 inflammasome and autophagy is a complex process. A limitation of our study was that we did not investigate the regulatory mechanisms between the NLRP3 inflammasome and autophagy under compressive force; thus, further exploration of the underlying mechanisms is required.

5 | CONCLUSIONS

Our study shows that mechanical force activates the NLRP3 inflammasome to regulate osteoclastogenesis via the cGAS/P2X7R/autophagy pathway (Figure 7). Our findings indicate that regulation of bone remodeling

during OTM is mediated through the prevention of excessive inflammasome activation or complete lack of inflammasome activation.

AUTHOR CONTRIBUTIONS

Contributed to the conception, design, data acquisition, analysis, and interpretation, drafted and critically revised the manuscript: Yineng Han. Contributed to data analysis and interpretation, and critically revised the manuscript: Qiaolin Yang and Yiping Huang. Contributed to critically revised the manuscript: Pengfei Gao and Lingfei Jia. Contributed to the conception, design, data acquisition, analysis, and interpretation, critically revised the manuscript: Weiran Li, Yunfei Zheng. All authors gave final approval and agreed to be accountable for all aspects of the work.

ACKNOWLEDGMENTS

This study was financially supported by the National Natural Science Foundation of China (No. 82071119, 82071142).

DISCLOSURES

The authors declare no potential conflicts of interest with respect to the authorship and publication of this article.

DATA AVAILABILITY STATEMENT

The data that support the findings of this study are available from the corresponding author upon reasonable request.

ORCID

Yunfei Zheng  <https://orcid.org/0000-0003-1899-8051>

Weiran Li  <https://orcid.org/0000-0001-9895-1143>

REFERENCES

- Miroshnikova YA, Le HQ, Schneider D, et al. Adhesion forces and cortical tension couple cell proliferation and differentiation to drive epidermal stratification. *Nat Cell Biol*. 2018;20(1):69-80. doi:10.1038/s41556-017-0005-z
- Hayakawa T, Yoshimura Y, Kikuri T, et al. Optimal compressive force accelerates osteoclastogenesis in RAW264.7 cells. *Mol Med Rep*. 2015;12(4):5879-5885. doi:10.3892/mmr.2015.4141
- Tan SD, de Vries TJ, Kuijpers-Jagtman AM, Semeins CM, Everts V, Klein-Nulend J. Osteocytes subjected to fluid flow inhibit osteoclast formation and bone resorption. *Bone*. 2007;41(5):745-751. doi:10.1016/j.bone.2007.07.019
- Kameyama S, Yoshimura Y, Kameyama T, et al. Short-term mechanical stress inhibits osteoclastogenesis via suppression of DC-STAMP in RAW264.7 cells. *Int J Mol Med*. 2013;31(2):292-298. doi:10.3892/ijmm.2012.1220
- Spyropoulou A, Karamesinis K, Basdra EK. Mechanotransduction pathways in bone pathobiology. *Biochim Biophys Acta*. 2015;1852(9):1700-1708. doi:10.1016/j.bbdis.2015.05.010
- He D, Kou X, Yang R, et al. M1-like macrophage polarization promotes orthodontic tooth movement. *J Dent Res*. 2015;94(9):1286-1294. doi:10.1177/0022034515589714
- Yan Y, Liu F, Kou X, et al. T cells are required for orthodontic tooth movement. *J Dent Res*. 2015;94(10):1463-1470. doi:10.1177/0022034515595003
- McCulloch CA, Lekic P, McKee MD. Role of physical forces in regulating the form and function of the periodontal ligament. *Periodontol 2000*. 2000;2000(24):56-72. doi:10.1034/j.1600-0757.2000.2240104.x
- Choi JW, Arai C, Ishikawa M, Shimoda S, Nakamura Y. Fiber system degradation, and periostin and connective tissue growth factor level reduction, in the periodontal ligament of teeth in the absence of masticatory load. *J Periodontol Res*. 2011;46(5):513-521. doi:10.1111/j.1600-0765.2011.01351.x
- Nakatsu S, Yoshinaga Y, Kuramoto A, et al. Occlusal trauma accelerates attachment loss at the onset of experimental periodontitis in rats. *J Periodontol Res*. 2014;49(3):314-322. doi:10.1111/jre.12109
- Gordon S. The macrophage: past, present and future. *Eur J Immunol*. 2007;37(Suppl 1):S9-S17. doi:10.1002/eji.200737638
- Feng X, Teitelbaum SL. Osteoclasts: new insights. *Bone Res*. 2013;1(1):11-26. doi:10.4248/BR201301003
- Horwood NJ. Macrophage polarization and bone formation: a review. *Clin Rev Allergy Immunol*. 2016;51(1):79-86. doi:10.1007/s12016-015-8519-2
- He D, Liu F, Cui S, et al. Mechanical load-induced H2S production by periodontal ligament stem cells activates M1 macrophages to promote bone remodeling and tooth movement via STAT1. *Stem Cell Res Ther*. 2020;11(1):112. doi:10.1186/s13287-020-01607-9
- Jin SS, He DQ, Wang Y, et al. Mechanical force modulates periodontal ligament stem cell characteristics during bone remodeling via TRPV4. *Cell Prolif*. 2020;53(10):e12912. doi:10.1111/cpr.12912
- Yum S, Li M, Fang Y, Chen ZJ. TBK1 recruitment to STING activates both IRF3 and NF-kappaB that mediate immune defense against tumors and viral infections. *Proc Natl Acad Sci U S A*. 2021;118(14):e2100225118. doi:10.1073/pnas.2100225118
- Gaidt MM, Ebert TS, Chauhan D, et al. The DNA inflammasome in human myeloid cells is initiated by a STING-cell death program upstream of NLRP3. *Cell*. 2017;171(5):1110-1124 e18. doi:10.1016/j.cell.2017.09.039
- Yang X, Chang HY, Baltimore D. Autoproteolytic activation of pro-caspases by oligomerization. *Mol Cell*. 1998;1(2):319-325. doi:10.1016/s1097-2765(00)80032-5
- Martinon F, Burns K, Tschopp J. The inflammasome: a molecular platform triggering activation of inflammatory caspases and processing of proIL-beta. *Mol Cell*. 2002;10(2):417-426. doi:10.1016/s1097-2765(02)00599-3
- Guarda G, Zenger M, Yazdi AS, et al. Differential expression of NLRP3 among hematopoietic cells. *J Immunol*. 2011;186(4):2529-2534. doi:10.4049/jimmunol.1002720
- Zang Y, Song JH, Oh SH, et al. Targeting NLRP3 inflammasome reduces age-related experimental alveolar bone loss. *J Dent Res*. 2020;99(11):1287-1295. doi:10.1177/0022034520933533
- Maruyama K, Nemoto E, Yamada S. Mechanical regulation of macrophage function—cyclic tensile force inhibits NLRP3 inflammasome-dependent IL-1beta secretion in murine macrophages. *Inflamm Regen*. 2019;39:3. doi:10.1186/s41232-019-0092-2
- Taddei SR, Moura AP, Andrade I Jr, et al. Experimental model of tooth movement in mice: a standardized protocol for studying bone remodeling under compression and

- tensile strains. *J Biomech.* 2012;45(16):2729-2735. doi:10.1016/j.jbiomech.2012.09.006
24. Han Y, Yang Q, Huang Y, et al. Mechanical force inhibited hP-DLSCs proliferation with the downregulation of MIR31HG via DNA methylation. *Oral Dis.* 2021;27(5):1268-1282. doi:10.1111/odi.13637
 25. Jiang N, He D, Ma Y, et al. Force-induced autophagy in periodontal ligament stem cells modulates M1 macrophage polarization via AKT signaling. *Front Cell Dev Biol.* 2021;9:666631. doi:10.3389/fcell.2021.666631
 26. Chen L, Mo S, Hua Y. Compressive force-induced autophagy in periodontal ligament cells downregulates osteoclastogenesis during tooth movement. *J Periodontol.* 2019;90(10):1170-1181. doi:10.1002/JPER.19-0049
 27. Mizushima N, Yoshimori T, Levine B. Methods in mammalian autophagy research. *Cell.* 2010;140(3):313-326. doi:10.1016/j.cell.2010.01.028
 28. Miller S, Oleksy A, Perisic O, Williams RL. Finding a fitting shoe for Cinderella: searching for an autophagy inhibitor. *Autophagy.* 2010;6(6):805-807. doi:10.1126/science.1184429
 29. Viecilli RF, Katona TR, Chen J, Hartsfield JK Jr, Roberts WE. Orthodontic mechanotransduction and the role of the P2X7 receptor. *Am J Orthod Dentofacial Orthop.* 2009;135(6):694 e1-694 e16; discussion 694-5. doi:10.1016/j.ajodo.2008.10.018
 30. Youm YH, Grant RW, McCabe LR, et al. Canonical Nlrp3 inflammasome links systemic low-grade inflammation to functional decline in aging. *Cell Metab.* 2013;18(4):519-532. doi:10.1016/j.cmet.2013.09.010
 31. Chen Y, Yang Q, Lv C, et al. NLRP3 regulates alveolar bone loss in ligature-induced periodontitis by promoting osteoclastic differentiation. *Cell Prolif.* 2021;54(2):e12973. doi:10.1111/cpr.12973
 32. Zhao D, Wu Y, Zhuang J, Xu C, Zhang F. Activation of NLRP1 and NLRP3 inflammasomes contributed to cyclic stretch-induced pyroptosis and release of IL-1beta in human periodontal ligament cells. *Oncotarget.* 2016;7(42):68292-68302. doi:10.18632/oncotarget.11944
 33. Li S, Li Q, Zhu Y, Hu W. GDF15 induced by compressive force contributes to osteoclast differentiation in human periodontal ligament cells. *Exp Cell Res.* 2020;387(1):111745. doi:10.1016/j.yexcr.2019.111745
 34. Danciu TE, Gagari E, Adam RM, Damoulis PD, Freeman MR. Mechanical strain delivers anti-apoptotic and proliferative signals to gingival fibroblasts. *J Dent Res.* 2004;83(8):596-601. doi:10.1177/154405910408300803
 35. Iwawaki Y, Mizusawa N, Iwata T, et al. MiR-494-3p induced by compressive force inhibits cell proliferation in MC3T3-E1 cells. *J Biosci Bioeng.* 2015;120(4):456-462. doi:10.1016/j.jbiosc.2015.02.006
 36. Chen Y, Mohammed A, Oubaidin M, et al. Cyclic stretch and compression forces alter microRNA-29 expression of human periodontal ligament cells. *Gene.* 2015;566(1):13-17. doi:10.1016/j.gene.2015.03.055
 37. Hopfner KP, Hornung V. Molecular mechanisms and cellular functions of cGAS-STING signalling. *Nat Rev Mol Cell Biol.* 2020;21(9):501-521. doi:10.1038/s41580-020-0244-x
 38. Katsnelson MA, Rucker LG, Russo HM, Dubyak GR. K⁺ efflux agonists induce NLRP3 inflammasome activation independently of Ca²⁺ signaling. *J Immunol.* 2015;194(8):3937-3952. doi:10.4049/jimmunol.1402658
 39. Di Virgilio F, Dal Ben D, Sarti AC, Giuliani AL, Falzoni S. The P2X7 receptor in infection and inflammation. *Immunity.* 2017;47(1):15-31. doi:10.1016/j.immuni.2017.06.020
 40. Albalawi F, Lu W, Beckel JM, Lim JC, McCaughey SA, Mitchell CH. The P2X7 receptor primes IL-1beta and the NLRP3 inflammasome in astrocytes exposed to mechanical strain. *Front Cell Neurosci.* 2017;11:227. doi:10.3389/fncel.2017.00227
 41. Cadwell K. Crosstalk between autophagy and inflammatory signalling pathways: balancing defence and homeostasis. *Nat Rev Immunol.* 2016;16(11):661-675. doi:10.1038/nri.2016.100
 42. Jacox LA, Tang N, Li Y, et al. Orthodontic loading activates cell-specific autophagy in a force-dependent manner. *Am J Orthod Dentofacial Orthop.* 2022;161(3):423-436 e1. doi:10.1016/j.ajodo.2020.09.034
 43. Li Y, Jacox LA, Coats S, et al. Roles of autophagy in orthodontic tooth movement. *Am J Orthod Dentofacial Orthop.* 2021;159(5):582-593. doi:10.1016/j.ajodo.2020.01.027
 44. Liu H, Huang Y, Yang Y, Han Y, Jia L, Li W. Compressive force-induced LincRNA-p21 inhibits mineralization of cementoblasts by impeding autophagy. *FASEB J.* 2022;36(1):e22120. doi:10.1096/fj.202101589R
 45. Allaes I, Marceau F, Poubelle PE. NLRP3 promotes autophagy of urate crystals phagocytized by human osteoblasts. *Arthritis Res Ther.* 2013;15(6):R176. doi:10.1186/ar4365
 46. Allaes I, Marceau F, Poubelle PE. NLRP3 promotes autophagy of urate crystals phagocytized by human osteoblasts. *Arthritis Res Ther.* 2013;15(6):R176. doi:10.1186/ar4365
 47. Lai M, Yao H, Shah SZA, et al. The NLRP3-caspase 1 inflammasome negatively regulates autophagy via TLR4-TRIF in prion peptide-infected microglia. *Front Aging Neurosci.* 2018;10:116. doi:10.3389/fnagi.2018.00116
 48. Kim SM, Kim YG, Kim DJ, et al. Inflammasome-independent role of NLRP3 mediates mitochondrial regulation in renal injury. *Front Immunol.* 2018;9:2563. doi:10.3389/fimmu.2018.02563
 49. Zhang Y, Sauler M, Shinn AS, et al. Endothelial PINK1 mediates the protective effects of NLRP3 deficiency during lethal oxidant injury. *J Immunol.* 2014;192(11):5296-5304. doi:10.4049/jimmunol.1400653
 50. Yu J, Nagasu H, Murakami T, et al. Inflammasome activation leads to Caspase-1-dependent mitochondrial damage and block of mitophagy. *Proc Natl Acad Sci U S A.* 2014;111(43):15514-15519. doi:10.1073/pnas.1414859111

SUPPORTING INFORMATION

Additional supporting information can be found online in the Supporting Information section at the end of this article.

How to cite this article: Han Y, Yang Q, Huang Y, et al. Compressive force regulates orthodontic tooth movement via activating the NLRP3 inflammasome. *The FASEB Journal.* 2022;36:e22627. doi: [10.1096/fj.202200447RR](https://doi.org/10.1096/fj.202200447RR)